ARTICLES
https://doi.org/10.1038/s41563-019-0548-4
nature materials

A transparent, self-healing and high-κ dielectric for low-field-emission stretchable optoelectronics

Yu Jun Tan[1,2], Hareesh Godaba[1,2,9], Ge Chen[1,9], Siew Ting Melissa Tan[2], Guanxiang Wan[1], Guojingxian Li[2], Pui Mun Lee[3], Yongqing Cai[4,8], Si Li[1], Robert F. Shepherd[5], John S. Ho[2,3,6] and Benjamin C. K. Tee[1,2,3,6,7]★

Stretchable optoelectronic materials are essential for applications in wearable electronics, human–machine interfaces and soft robots. However, intrinsically stretchable optoelectronic devices such as light-emitting capacitors usually require high driving alternating voltages and excitation frequencies to achieve sufficient luminance in ambient lighting conditions. Here, we present a healable, low-field illuminating optoelectronic stretchable (HELIOS) device by introducing a transparent, high permittivity polymeric dielectric material. The HELIOS device turns on at an alternating voltage of 23 V and a frequency below 1 kHz, safe operating conditions for human–machine interactions. We achieved a brightness of 1,460 cd m^{-2} at 2.5 V µm^{-1} with stable illumination demonstrated up to a maximum of 800% strain. The materials also self-healed mechanically and electronically from punctures or when severed. We further demonstrate various HELIOS light-emitting capacitor devices in environment sensing using optical feedback. Moreover, our devices can be powered wirelessly, potentially enabling applications for untethered damage-resilient soft robots.

The swift development of electronic skins[1–4], wearable electronics[5] and soft robots[6,7] have spurred widespread research interest in the development of new formats for optical displays that are highly stretchable, conformable and capable of displaying optical information[8]. For instance, stretchable electroluminescent (EL) devices can be used in bio-inspired soft robots that navigate obstacles and perform optical communication[9].

Stretchable optoelectronic displays require two key components: (1) a light-emitting source and (2) compatible stretchable substrates. Several emission mechanisms have been explored to achieve EL displays, such as light-emitting diodes (LEDs)[10] and high-field a.c. EL devices[6,11,12]. LEDs have excellent performance at low operating voltages using careful interfacial engineering of electron–hole junctions[10]. However, because LEDs are not intrinsically stretchable, extrinsic designs that connect LEDs on substrates with stretchable electrodes are necessary[10,13–16].

On the other hand, EL phosphors are used in stretchable light-emitting capacitors (LECs) by incorporating them into an elastomer. The light emitting layer (dielectric-EL) is sandwiched in between two stretchable electrodes. The LEC devices can provide uniform light emission over their entire surface, as compared to light sources such as LEDs. However, previously demonstrated stretchable LECs require high a.c. electric fields (E) to excite luminescent centres, because of the low dielectric permittivity (κ) of the elastomers used. They also require high frequencies (f_{ac}) in the kilohertz range to reach sufficiently high luminance[6,17]. These electrical operating conditions pose challenges to portability, as well as in applying these devices safely and quietly[18] for human–machine interactions. High applied alternating voltages (V_{ac}), high f_{ac} and the physical damage that results from use also limit their operating lifetimes. Hence, a low operating E and f_{ac}, as well as self-healing capabilities, are critical and highly desirable for LEC applications[19,20].

Here, we introduce a HELIOS LEC device using a high-κ, transparent elastomeric dielectric material. Our high-κ dielectric significantly reduces the E, V_{ac} and f_{ac} required for safely achieving daylight-visible luminance of an LEC. We also found that the HELIOS device exhibits repeatable, autonomous self-healing from physical damage to its optical and mechanical properties.

Design and fabrication of HELIOS device

Previous LEC systems focused on the use of stretchable electrode materials[17] but did not address the high V_{ac} (and E) needed to achieve electroluminance. To significantly lower the E required, we present a strategy that incorporates a highly transparent high-κ dielectric-EL composite layer sandwiched between a pair of transparent electrodes[13] (Fig. 1a). Optical transparencies of the electrode and the dielectric are in the ranges 94–100% and 80–97% in the visible light wavelengths, respectively (Supplementary Fig. 1). We observed that EL phosphor particles dispersed well within the dielectric matrix (Supplementary Fig. 2).

We chose a poly(vinylidene fluoride) (PVDF)-based fluoroelastomer as the dielectric matrix material due to their high κ values[21]. To enhance the maximum strain that can be applied to the polymer, we added a small amount of non-ionic fluorinated surfactant to the high-κ fluoroelastomer (Methods). The resulting soft dielectric demonstrated intrinsic self-healing properties and enhanced κ.

[1]Department of Materials Science and Engineering, National University of Singapore, Singapore, Singapore. [2]Institute of Innovation in Health Technology (iHealthtech), National University of Singapore, Singapore, Singapore. [3]Electrical and Computer Engineering, National University of Singapore, Singapore, Singapore. [4]Institute Of High Performance Computing, Agency for Science Technology and Research, Singapore, Singapore. [5]Mechanical & Aerospace Engineering, Cornell University, Ithaca, NY, USA. [6]N.1 Institute of Health, National University of Singapore, Singapore, Singapore. [7]Institute of Materials Research and Engineering, Agency for Science Technology and Research, Singapore, Singapore. [8]Present address: Joint Key Laboratory of the Ministry of Education, Institute of Applied Physics and Materials Engineering, University of Macau, Avenida da Universidade, Taipa, Macau, China. [9]These authors contributed equally: Hareesh Godaba, Ge Chen. *e-mail: benjamin.tee@nus.edu.sg

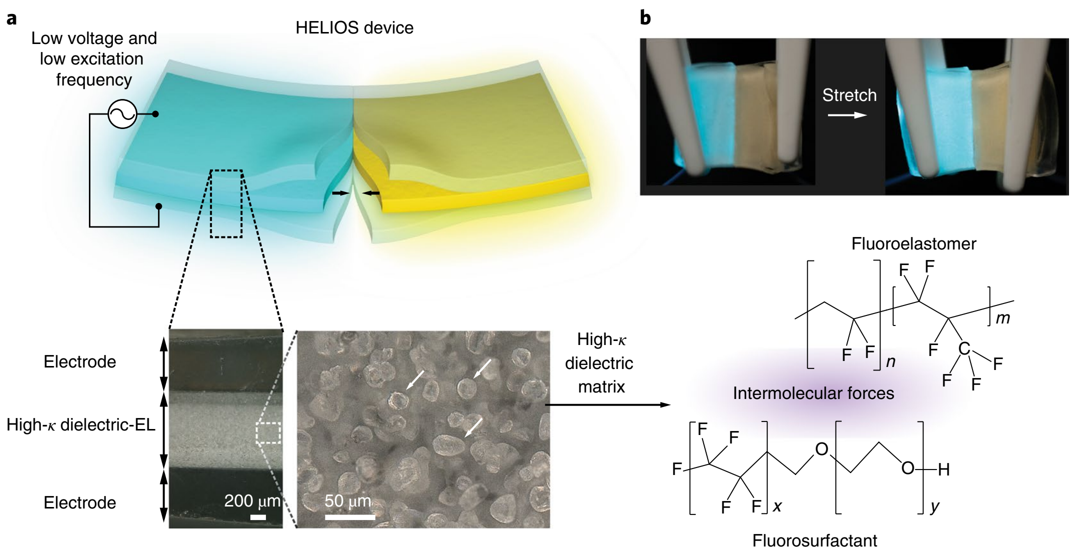

Fig. 1 | Design of the HELIOS optoelectronic device. a, Schematic illustrating the HELIOS device architecture. The entire device is intrinsically self-healable and highly stretchable. Optical micrographs below show the three-layered HELIOS structure. White arrows indicate phosphor particles. The high-κ dielectric matrix consists of a fluoroelastomer with non-ionic fluorinated surfactants. The reversible bonds between the molecules can be broken and reformed in ambient conditions. **b**, Photographs demonstrate that the orange and blue HELIOS devices can reconfigure and heal into one device at ambient environmental conditions. The device functions when strained after self-healing.

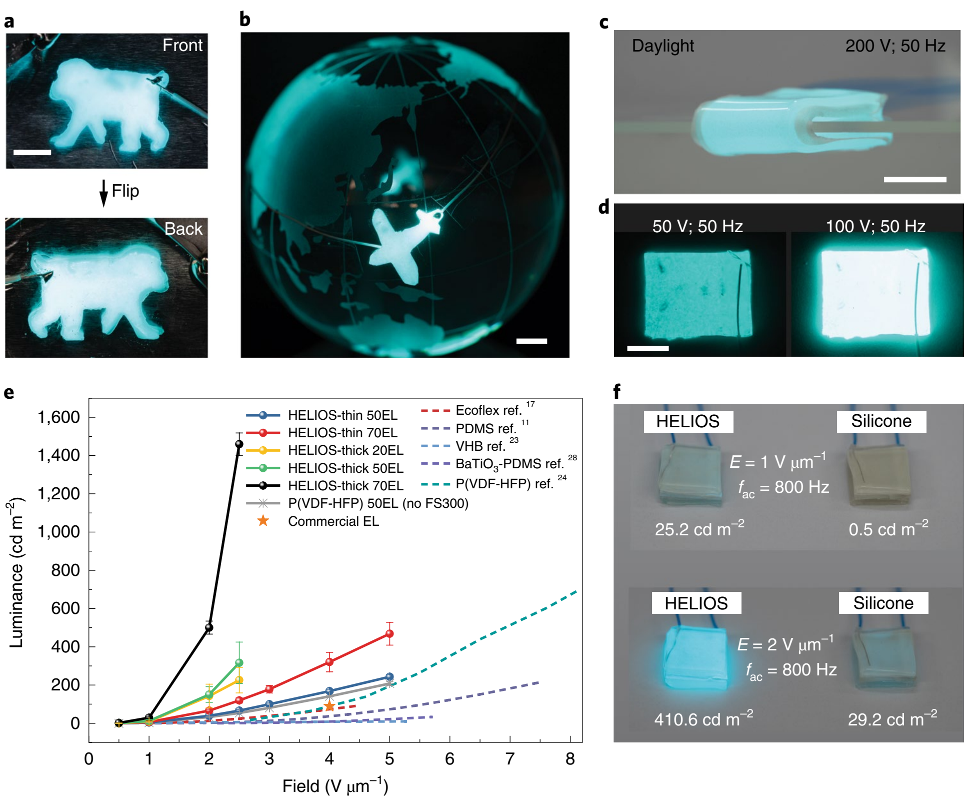

Fig. 2 | Shape reconfigurability and low emission voltage of the conformable HELIOS optoelectronic device. a, Photographs showing a patterned HELIOS device fabricated by mechanically punching out desired geometries. Both sides of the device can illuminate. Scale bar, 5 mm. **b**, Optical photograph showing that a cut HELIOS device provides all-angle illumination. Scale bar, 5 mm. **c**, Photograph showing a HELIOS device conforming to the edge of a glass slide of 1 mm thickness. Scale bar, 5 mm. **d**, Photographs of the HELIOS device working at a V_{ac} of 50 V ($E = 0.8$ V μm^{-1}) and of 100 V ($E = 1.5$ V μm^{-1}). Scale bars, 5 mm. **e**, A comparison of the devices in this work to prior reported stretchable LECs in terms of applied fields and their corresponding luminance. The measurements obtained from this work were reproduced with three samples for each condition, and the error bars represent the standard deviation. **f**, Photographs comparing samples of ~1.5 mm thickness of the HELIOS-thick and silicone (Ecoflex) LECs in daylight. Sample dimensions, 10 mm × 10 mm. VHB, Very High Bond.

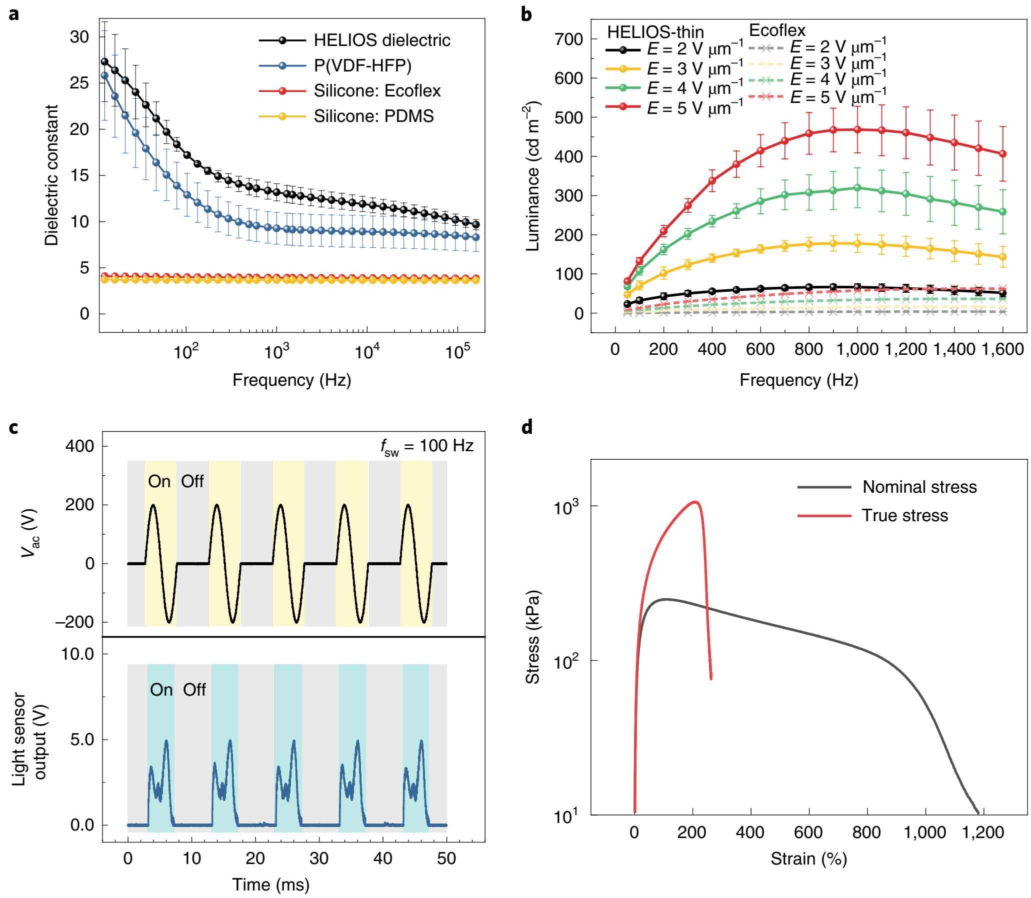

Fig. 3 | Electro-mechanical properties of the HELIOS materials and the HELIOS LEC device. a, Dielectric constants of the HELIOS dielectric compared to other stretchable materials. The control materials have much lower dielectric constants, which results in high activation voltages and excitation frequencies in these LECs. The error bars depict the standard deviation from three samples. **b**, Graph showing luminance of HELIOS device and a control device operated at $E = 2$, 3, 4 and 5 V μm^{-1} and varying frequencies. The measurements were reproduced on three samples, and the error bars represent the standard deviation. **c**, Graphs showing the f_{sw} response from a photodiode signal of the HELIOS device (bottom) when operated with f_{sw} of 100 Hz and f_{ac} of 200 Hz (top). **d**, The uniaxial tensile behaviour of the HELIOS dielectric material.

Our proposed combination is different from that in previous work, which had incorporated ionic liquids to make conductive self-healing ionogels[13,22]. Although these ionic-based additives enhance the κ of the materials, they cannot be used as the insulating dielectric layer in LECs, because the ionic conductivity under V_{ac} will lead to leakage currents that reduce the capacitive effects needed for light emission.

Moreover, our design allows all three layers of HELIOS LEC devices to be self-healable. Self-healing of HELIOS devices enables rapid reconfigurability: separate halves of the blue (ZnS:Cu) and orange (ZnS:Cu,Mn) devices can be conveniently merged into one device (Fig. 1b). Our dielectric is highly surface compatible with the electrodes, as it adheres to the electrodes without using any adhesive or surface treatment (Supplementary Fig. 3a,b). Therefore, device fabrication is facile and does not require significant interfacial engineering.

The HELIOS device can be 3D printed, enabling the patterning of different display designs (Supplementary Fig. 4a,b). The soft nature of the electrodes and high-κ dielectric-EL allows it to be readily configured by mechanical die punching or cutting into desirable shapes (Fig. 2a,b, Supplementary Fig. 4c,d). The HELIOS device can illuminate even when flexed to a 0.5 mm radius of curvature at the edge of a glass slide (Fig. 2c).

We categorize our device into three classes according to dielectric-EL thickness: HELIOS-thin (dielectric-EL thickness, $t \leq 200$ μm), HELIOS-mid (200 μm $< t <$ 1 mm) and HELIOS-thick ($t \geq 1$ mm). The high-κ dielectric allows the HELIOS-thin device to turn on at voltages as low as $V_{ac} = 23$ V ($E = 0.3$ V μm^{-1}) (Supplementary Fig. 5a) and achieves high luminance at V_{ac} of 40–100 V (Fig. 2d, Supplementary Fig. 5b–d).

We compared the luminance values at different E with those of state-of-the-art, intrinsically stretchable LECs (Fig. 2e and Supplementary Table 1) that use dielectric materials from silicones, such as polydimethylsiloxane (PDMS)[11] and Ecoflex[6,17]; acrylic elastomers, such as those used in VHB (Very High Bond) tapes[23]; or PVDF-based elastomers[24] as the dielectric layer. The luminance of HELIOS-thin exceeds the performance of other stretchable LEC devices reported in the literature across a wide range of E (refs. [23,24]). In addition, we show that the brightness of the HELIOS-thin device is comparable to the maximum brightness setting of a smartphone display (270 cd m^{-2}) in a daylight environment at V_{ac} of 200 V ($E = 2$ V μm^{-1}) (Supplementary Video 1). In contrast, silicone-based stretchable LECs had a luminance that is imperceptible to human eyes at the same E and f_{ac}. We also compared thick LEC devices; the HELIOS-thick device was much brighter than a silicone-based LEC at 1,500 V ($E = 1$ V μm^{-1}) and 3,000 V ($E = 2$ V μm^{-1}) (Fig. 2f).

Electrical properties and performance of dielectric

The HELIOS dielectric material has a high κ value between 10 and 27, which is 2.5- to 6.8-fold higher than silicones across the

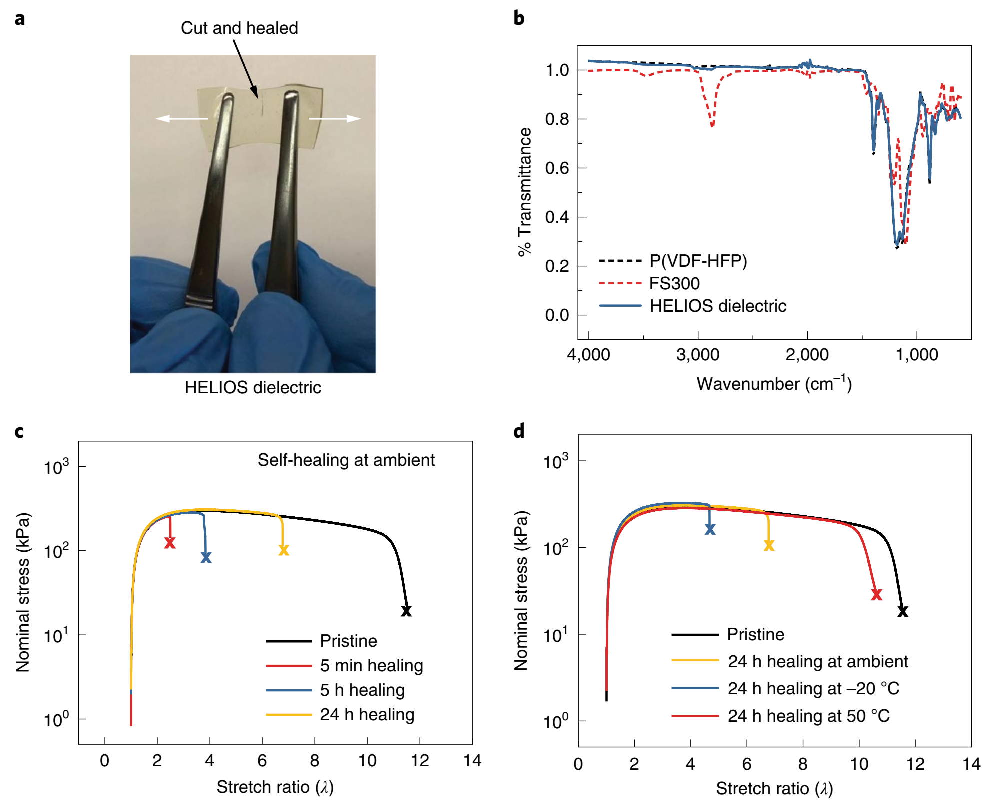

Fig. 4 | Self-healing of the HELIOS dielectric material. a, Photograph of the self-healed HELIOS dielectric. **b**, FTIR spectra of P(VDF-HFP), FS300 and HELIOS dielectric. **c**,**d**, Self-healing in mechanical properties of the HELIOS dielectric at room temperature (**c**) and at −20 °C, room temperature and 50 °C (**d**). The x denotes the failure point of the material.

same frequency range (Fig. 3a). Using density functional theory (DFT), we calculated the dipole moments of the fluoroelastomer and the fluorosurfactant (FS300) to be 3.22 and 2.83 D, respectively (Supplementary Fig. 6a). Within the fluoroelastomer matrix, FS300 molecules improve the κ in the HELIOS dielectric material through the realignment of these dipole centres upon exposure to an electric field. The κ value decreases with increasing frequency due to the frequency-dependent interfacial polarization effects[25]. The high-κ effectively raises the E across the EL particles (Supplementary Fig. 6b), which obviates the need for a high applied E. Using silicone-based devices as controls, we demonstrated that the HELIOS device is significantly brighter under the same operating conditions (Fig. 3b, Supplementary Figs. 6c–9). Moreover, the HELIOS device has a luminous efficacy of 1.26 lm W^{-1} (and the lowest power consumption, at ~4.6 mW), which compares favourably to other stretchable LEC devices[6,24].

Low V_{ac} and f_{ac}

An approach to reduce the turn-on threshold voltage is to use thin dielectric-EL layers. In fact, most of the demonstrated LECs use a thin dielectric-EL layer ($t = 10$ to 100 μm). Despite this, such LEC devices using low κ materials still required a high turn-on V_{ac} (>100 V)[11,17]. Here we show that our HELIOS-thin device turns on at a V_{ac} of 23 V.

In addition, HELIOS LECs required a lower f_{ac} than the reported stretchable LECs. The HELIOS device flickered at f_{ac} lower than 50 Hz and remained steadily illuminated beyond 50 Hz because the light emission rate is beyond the human flicker fusion rate[26]. The low f_{ac} does not imply a slow switching frequency (f_{sw}) or a turn-on delay. The HELIOS LEC device can switch on and off at the same f_{sw}, regardless of the f_{ac} provided to the device (Fig. 3c and Supplementary Fig. 10). The turn-on delay of the device falls in the range of hundreds of nanoseconds (Supplementary Table 2). When using a low f_{ac} of 50 Hz on the HELIOS-thin device, we achieved luminance of 5 cd m^{-2} at V_{ac} of 100 V ($E = 1.6$ V μm^{-1}). This brightness value is within the low brightness setting of a typical smartphone display luminance (2–10 cd m^{-2}).

A low f_{ac} enables convenient operation of the device, as the frequency of most domestic power supplies is either 50 or 60 Hz (and at 110 or 220 V). For most of the commercially available LEC devices, the f_{ac} required is in the range of kilohertz. The devices cannot be illuminated at 50 or 60 Hz unless a high V_{ac} is also applied. Transformers and inverters that produce voltages with f_{ac} in the kilohertz range cause an audible whining noise. As HELIOS LECs do not require a kilohertz excitation frequency for illumination, the circuit can be simpler and quieter. Moreover, operation at low f_{ac} can help increase the LEC devices' lifetimes[27].

Luminance enhancement

In general, the brightness of HELIOS LECs increases with a high E and f_{ac}, but peaks at a certain f_{ac} for a constant E (Supplementary Fig. 5c). The luminance of LEC devices can be enhanced by using a higher concentration of phosphor particles in the dielectric layer. We used three concentrations of phosphor particles for comparison: 20EL (20 wt%, equivalent to 9.1 v./v.% of phosphor particles in the HELIOS dielectric), 50EL (50 wt%, 28.7 v./v.%) and 70EL (70 wt%, 48.4 v./v.%). The luminance of 70EL is almost double the luminance of 50EL at various operating conditions (Supplementary Fig. 11a). The increment is due to the dual effect of higher phosphor particle density per unit area coupled with a significant concentration of E energy on each particle (Supplementary Fig. 11b). While the use of high-κ ceramic particles such as barium titanate ($BaTiO_3$) can improve the κ of the resultant composite[28], the reduction in the volume fraction of phosphor particles dispersed inevitably affects the luminance. Figure 2e shows that such a composite's brightness did not surpass those of the rest of our LEC systems.

To further increase the brightness of LEC devices, we used a thick dielectric-EL layer to achieve a higher phosphor concentration per unit area (Supplementary Figs. 12 and 13). At the same applied E and f_{ac}, the luminance of the HELIOS 50EL device improved by 3.5 times as t increased from 100 μm to 500 μm. We measured an unprecedented LEC brightness of 1,460 cd m^{-2} (V_{ac} = 3750 V; E = 2.5 V μm^{-1}; f_{ac} = 800 Hz) (Extended Data Fig. 1, Supplementary Fig. 14) for HELIOS-thick 70EL. This is 12.4 times the brightness of the HELIOS-thin 70EL and 22 times the brightness of the HELIOS-thin 50EL at the same operating E and f_{ac}. The luminance of the HELIOS-thick devices was much brighter than the thick, elastomer-based control devices across the tested conditions (Supplementary Fig. 15). In addition, we measured comparable luminance values for the HELIOS-thick device even after three months under ambient storage (Supplementary Fig. 16).

Mechanical performance

The HELIOS dielectric can be described as a supramolecular polymer[29] (Extended Data Fig. 2a,b) that can be stretched elastically up to 20% with Young's modulus of 1.06 ± 0.08 MPa and that deforms plastically to 906 ± 58% (Fig. 3d, Supplementary Video 2). Its ultimate tensile strength is 0.21 ± 0.10 MPa (computed true strength, 1.03 ± 0.02 MPa).

The HELIOS electrodes and dielectric-EL have highly compatible interfaces and mechanical properties, which help to minimize interfacial discontinuities and eliminate slipping or delamination in multi-layered devices such as our HELIOS LEC devices. The interfacial bonding between the HELIOS electrode and HELIOS dielectric-EL was much stronger than that between the controls of a HELIOS electrode and silicone dielectric, or between typical transparent electrodes such as indium tin oxide/polyethylene terephthalate (ITO/PET) electrodes and a HELIOS dielectric-EL (Supplementary Fig. 3, Supplementary Video 3). Both the dielectric-EL composite and the three-layered HELIOS device (electrode/dielectric-EL/electrode) recovered to their original lengths even after multiple cycles of stretching to 50% strain (Extended Data Fig. 2c,d).

While a low turn-on voltage can be achieved when using thin dielectric-EL layers, the maximum strain of the LEC device will be modest because the two electrodes eventually contact each other as the strained dielectric layer becomes too thin (Extended Data Fig. 3a). Conversely, a thicker dielectric-EL layer can enable operation at larger mechanical strains, but activation voltage increases. Previously described LECs with a thick dielectric-EL layer (~1 mm) were highly stretchable (>480% strain), but they require a significantly high V_{ac} of 2.5 kV (E = 2.5 V μm^{-1}, f_{ac} = 700 Hz) for light emission[6,30].

Instead, using our high-κ dielectric HELIOS-thick 20EL device achieved an adequate human-perceivable brightness of 3.7 cd m^{-2} at 800 V (E = 0.8 V μm^{-1}, f_{ac} = 50 Hz; Extended Data Fig. 3b) at a similar dielectric-EL thickness of ~1 mm. When operating at 800 V and 50 Hz, the HELIOS LEC can be stretched to ~800% strain with stable light emission (Extended Data Fig. 3c). The brightness of the HELIOS device initially increases with the strain (up to ~400% strain) due to the increase in the E as the dielectric sandwiched between electrodes decreases in thickness under uniaxial tension. However, when stretched beyond five times its original length, the formation of conductive paths between the electrodes reduces the effective capacitance (Supplementary Fig. 17a).

We further demonstrate the elasticity enhancement of the HELIOS device via two strategies: (1) encapsulating the device within an elastomer and (2) cross-linking the dielectric. Due to the conformality of the HELIOS device, we can form wavy devices and then encapsulate them in elastomers as a strategy to improve the device elasticity (Supplementary Note 1). The encapsulated device can be stretched for 200 cycles without observable changes in shape and performance. Alternatively, we show that cross-linking of the dielectric material can inherently enhance the rubbery characteristics of the material (Supplementary Note 2). Although the cross-linked HELIOS dielectric is not as transparent as the HELIOS dielectric, the cross-linked HELIOS-thin device can achieve higher luminance than the pristine HELIOS-thin device due to the increase in the κ value of the cross-linked HELIOS dielectric material. After 200 stretch cycles, the mechanical and luminance properties of the cross-linked HELIOS device were comparable to those of the pristine device.

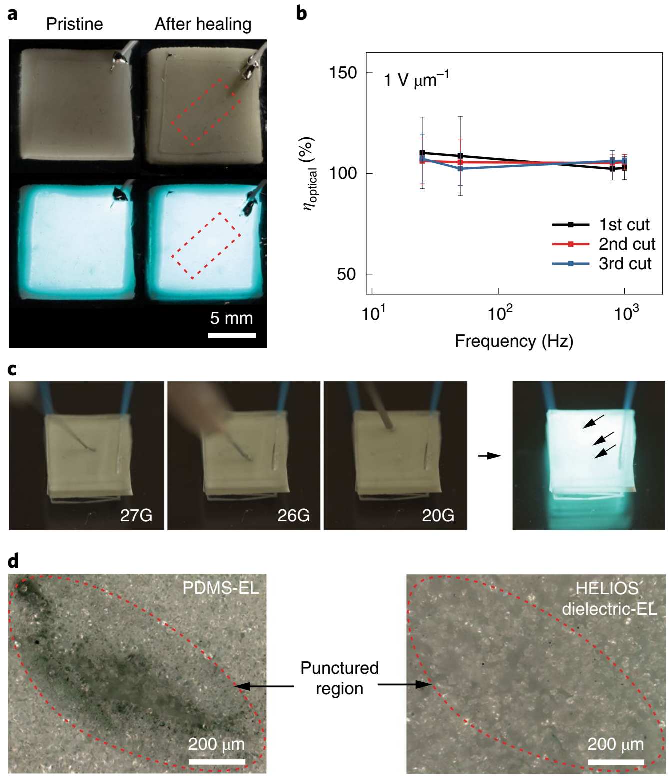

Fig. 5 | Self-healing of the HELIOS materials and the optoelectronic device. **a**, Photographs showing that the damaged HELIOS LEC can re-illuminate immediately after placing the interfaces together and applying gentle pressure. Red rectangle indicates the cut and healed region of the sample. **b**, Self-healing of the luminance of the HELIOS device with three subsequent cuts and healing at ambient environmental conditions. **c**, Photographs showing that the HELIOS device can re-illuminate with no waiting time for healing after multiple punctures. 27G, 26G and 20G represent the nominal outer diameters of the needles of 0.41 mm, 0.46 mm and 0.91 mm, respectively. Arrows show the scars from the punctures. **d**, Optical micrographs comparing the dielectric-EL composite with the PDMS-EL dielectric being punctured. In the HELIOS dielectric-EL composite, the punctured hole diminished in size after a gentle pressing, whereas the PDMS-EL ruptured permanently.

Self-healing properties

When we mechanically pressed two freshly damaged interfaces of the dielectric material together, the interfaces merged and self-healed (Fig. 4a). Notably, the self-healing dielectric material is not tacky on its surface (Supplementary Fig. 3c and Supplementary Videos 3 and 4).

The amorphous HELIOS dielectric material has an extremely low glass transition temperature, T_g (−25 °C) (Supplementary Fig. 17b), so the polymer chains are fairly mobile at ambient conditions. Upon addition of the FS300 to the fluoroelastomer, results from

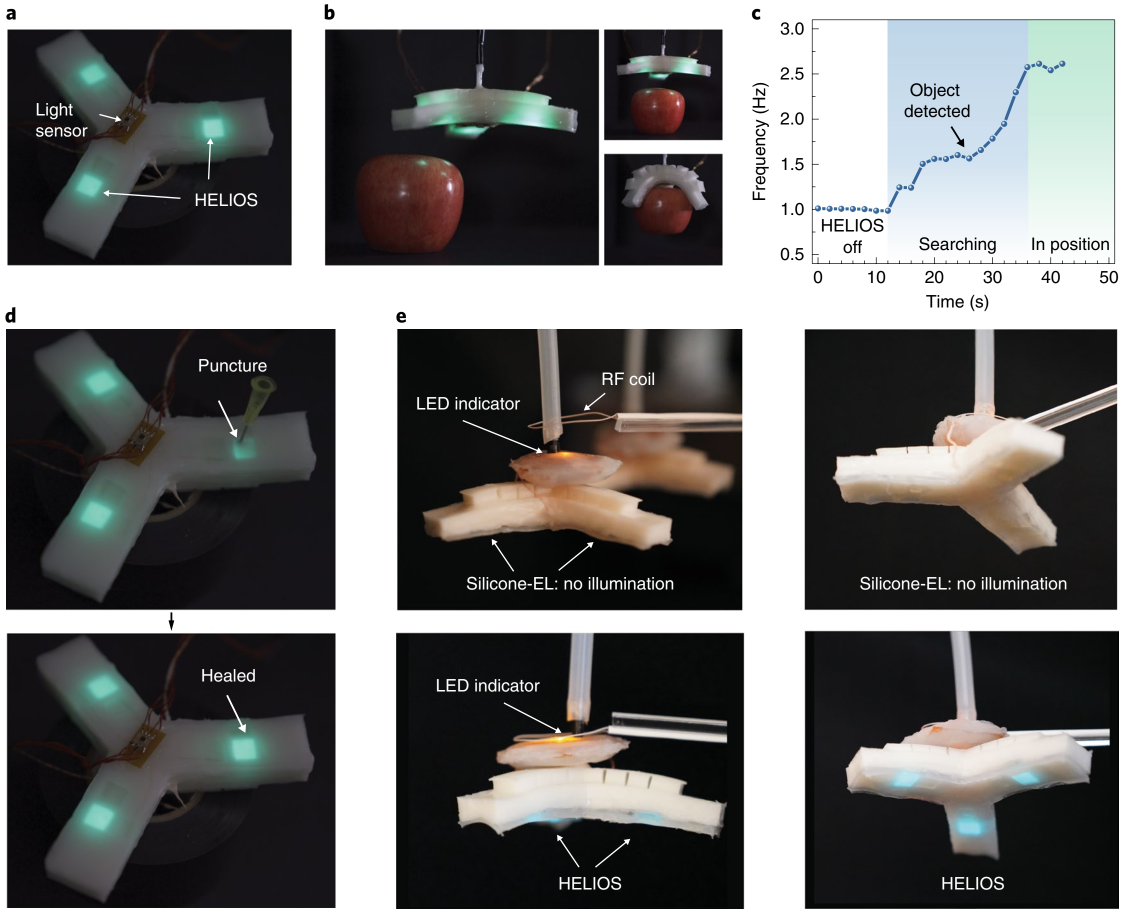

Fig. 6 | HELIOS-equipped soft robots. a, Photograph showing a soft gripper with HELIOS devices and light sensor. **b**, Surveillance in the dark of soft gripper with HELIOS devices near an apple and subsequently picking up the apple. **c**, Graph showing the signal from the light sensor while detecting the position of the apple. **d**, Photographs showing the HELIOS device healed immediately after a puncture. **e**, Photographs of an LEC soft gripper that can be powered wirelessly. The HELIOS LEC devices can illuminate using wireless power transfer. On the other hand, a similarly constructed silicone-EL control device could not illuminate because of the high operating voltages required. RF, radiofrequency.

attenuated total reflectance Fourier transform infrared spectroscopy (FTIR-ATR) show a peak appearance at 1,639 cm^{-1} and multiple peaks shifts, which suggest synergistic intermolecular interactions between the polymer chain and the surfactant (Fig. 4b and Supplementary Note 3).

These observations are consistent with our DFT calculations (Supplementary Note 4). The FS300 tends to have a strong interaction with the fluoroelastomer ascribed to its fluorine groups. The abundant fluorine in the fluoroelastomer/FS300 system allows rich hydrogen–fluorine intermolecular bond (–H…F–) pairing including the strong dipole–dipole and van der Waals interactions. A differential charge density calculation of the molecular hybrids also clearly shows stronger charge fluctuations in the backbone of the FS300, implying a strong interaction with the fluoroelastomer. These reversible non-covalent bonds can be repeatedly broken and reformed, giving rise to the repeatable self-healing capability.

We characterized the self-healing properties of the HELIOS dielectric specimens on tensile bars (Supplementary Video 5). After bifurcating the specimen in the middle, we repositioned the two parts back together with a gentle compressive force (~0.08 N). The dielectric material showed rapid self-healing. After just 5 min of healing at ambient conditions, 91% of the ultimate tensile strength of the pristine material was recovered (Fig. 4c), and the material healed almost completely (toughness recovered by 91%) in one day when heated to 50 °C (Fig. 4d). Remarkably, the material can also heal at −20 °C due to the low T_g of the material (−25 °C). Self-healing of the material improves with an increase in healing time and temperature. Additionally, when the surface area for healing is increased in thicker samples, alignment of the self-heal region is much easier and the number of bonds for self-healing increases, and more rapid healing at room temperature can be achieved (Supplementary Video 6).

Luminance damage resiliency

HELIOS devices exhibited recovery of optical performance in addition to mechanical healing (Supplementary Note 5). We cut a pristine HELIOS device through all three device layers and gently pressed the damaged surfaces together. After 5 min, the HELIOS device retains its luminance and the damaged interface region emits light (Fig. 5a), albeit with a vaguely visible scar (Supplementary Fig. 18a).

We define the luminance self-healing efficiency as η_{optical}, which is the percentage of luminance restored relative to the original luminance. The average η_{optical} ranged from 89 to 128% (Fig. 5b and Supplementary Fig. 18b). These changes in luminance can be attributed to the inevitable but slight change in the dielectric thickness and optical scattering effects during the manual damage-and-heal processes.

In addition, the HELIOS dielectric is puncture-resilient when piercing with a conducting (Fig. 5c, Supplementary Fig. 19 and Supplementary Video 7) or an insulating needle (Supplementary Fig. 20). The main reason for the puncture resistance of the HELIOS device is the low V_{ac} and f_{ac} needed by the device to achieve the same brightness as the silicone control. In addition, the HELIOS dielectric can heal from mechanical damage due to its intrinsic self-healing property (Fig. 5d).

Soft robot applications with the HELIOS device

We embedded the HELIOS LECs into a prototypical soft robotic gripper capable of receiving optical feedback, using a previously described self-sealing soft robotic gripper[31]. The embedded HELIOS LECs act as flexible light sources. Together with an optical sensing photodetector integrated to the gripper base, a HELIOS-equipped gripper can be used to sense the proximity of objects in dark environments. As the gripper approaches a target object, the light intensity reflected from the object increases. This indicates the object's proximity and signals the pneumatic actuator to grasp the target (Fig. 6a–c and Supplementary Video 8).

The robustness of our HELIOS LECs to needle punctures (Fig. 6d and Supplementary Video 9) enables the soft robotic gripper to grasp sharp objects. We pneumatically actuated the soft robotic gripper to conform to an inflated balloon and intentionally pierced a needle through the gripper and the HELIOS device until it punctured the balloon. The robotic gripper instantly self-healed both mechanically and optically.

HELIOS LEC devices incorporated in soft grippers can be wirelessly powered using off-the-shelf electronics (Fig. 6e, Supplementary Fig. 21 and Supplementary Video 10). With a radiofrequency coil transmitter, we illuminated the HELIOS-equipped gripper ($V_{ac}=50$ to 90 V, $f_{ac}=200$ Hz). By contrast, a similarly made silicone-EL gripper did not illuminate. These wirelessly powered optoelectronic devices could be useful for emerging resilient untethered soft robots[32].

Outlook

In summary, we introduced a HELIOS device that has the lowest turn-on threshold voltage and excitation frequency of all the stretchable LECs reported. The addition of an appropriate fluorosurfactant in the fluoroelastomer significantly lowered the electronic voltages and excitation frequencies required of the LECs, enhancing portability and reducing the associated noise during operation. The self-healing property of the device affords robustness and increases resilience against unexpected damage events, especially in autonomous robotic applications where manual repair could be unfeasible. Although the HELIOS dielectric material is elastic up to 20%, we showed its elasticity can be further enhanced by physical or chemical strategies.

The low driving E and f_{ac} of HELIOS LEC devices will further enable miniaturization and autonomous soft machines using miniature on-board microelectronics. For example, we demonstrated the use of wirelessly powered HELIOS LEC devices in damage-robust soft robotic grippers with optical feedback. We anticipate that our work can provide unique and robust optoelectronic building blocks for emerging soft machines[33], human–machine interfaces and wearable displays.

Online content

Any methods, additional references, Nature Research reporting summaries, source data, extended data, supplementary information, acknowledgements, peer review information; details of author contributions and competing interests; and statements of data and code availability are available at https://doi.org/10.1038/s41563-019-0548-4.

Received: 15 November 2018; Accepted: 30 October 2019;
Published online: 16 December 2019

References

1. Tee, B. C. K. et al. A skin-inspired organic digital mechanoreceptor. *Science* **350**, 313–316 (2015).
2. Yokota, T. et al. Ultraflexible organic photonic skin. *Sci. Adv.* **2**, e1501856–e1501856 (2016).
3. Hammock, M. L., Chortos, A., Tee, B. C. K., Tok, J. B. H. & Bao, Z. 25th anniversary article: the evolution of electronic skin (e-skin): a brief history, design considerations, and recent progress. *Adv. Mater.* **25**, 5997–6038 (2013).
4. Sekitani, T. & Someya, T. Stretchable, large-area organic electronics. *Adv. Mater.* **22**, 2228–2246 (2010).
5. Chou, H.-H. et al. A chameleon-inspired stretchable electronic skin with interactive colour changing controlled by tactile sensing. *Nat. Commun.* **6**, 8011 (2015).
6. Larson, C. et al. Highly stretchable electroluminescent skin for optical signaling and tactile sensing. *Science* **351**, 1071–1074 (2016).
7. Lu, N. & Kim, D.-H. Flexible and stretchable electronics paving the way for soft robotics. *Soft Robot.* **1**, 53–62 (2014).
8. Kim, R.-H. et al. Waterproof AlInGaP optoelectronics on stretchable substrates with applications in biomedicine and robotics. *Nat. Mater.* **9**, 929–937 (2010).
9. Shepherd, R. F. et al. Multigait soft robot. *Proc. Natl Acad. Sci. USA* **108**, 20400–20403 (2011).
10. Sekitani, T. et al. Stretchable active-matrix organic light-emitting diode display using printable elastic conductors. *Nat. Mater.* **8**, 494–499 (2009).
11. Wang, J., Yan, C., Chee, K. J. & Lee, P. S. Highly stretchable and self-deformable alternating current electroluminescent devices. *Adv. Mater.* **27**, 2876–2882 (2015).
12. Kim, E. H. et al. Organic light emitting board for dynamic interactive display. *Nat. Commun.* **8**, 14964 (2017).
13. Cao, Y. et al. Self-healing electronic skins for aquatic environments. *Nat. Electron* **2**, 75–82 (2019).
14. Sekitani, T. et al. A rubberlike stretchable active matrix using elastic conductors. *Science* **321**, 1468–1472 (2008).
15. Etienne, P. et al. Self-healing stretchable wires for reconfigurable circuit wiring and 3D microfluidics. *Adv. Mater.* **25**, 1589–1592 (2013).
16. Yin, D. et al. Efficient and mechanically robust stretchable organic light-emitting devices by a laser-programmable buckling process. *Nat. Commun.* **7**, 11573 (2016).
17. Wang, J. et al. Extremely stretchable electroluminescent devices with ionic conductors. *Adv. Mater.* **28**, 4490–4496 (2016).
18. Yen, W. M., Shionoya, S. & Yamamoto, H. (eds) *Phosphor Handbook* 2nd edn (CRC Press/Taylor and Francis Group, 2006).
19. Tan, Y. J., Wu, J., Li, H. & Tee, B. C. K. Self-healing electronic materials for a smart and sustainable future. *ACS Appl. Mater. Interfaces* **10**, 15331–15345 (2018).
20. Wallin, T. J., Pikul, J. & Shepherd, R. F. 3D printing of soft robotic systems. *Nat. Rev. Mater.* **3**, 84–100 (2018).
21. Ribeiro, C. et al. Electroactive poly(vinylidene fluoride)-based structures for advanced applications. *Nat. Protoc.* **13**, 681–704 (2018).
22. Cao, Y. et al. A transparent, self-healing, highly stretchable ionic conductor. *Adv. Mater.* **29**, 1605099 (2017).
23. Yang, C. H., Chen, B., Zhou, J., Chen, Y. M. & Suo, Z. Electroluminescence of giant stretchability. *Adv. Mater.* **28**, 4480–4484 (2016).
24. Zhou, Y. et al. Bright stretchable electroluminescent devices based on silver nanowire electrodes and high-k thermoplastic elastomers. *ACS Appl. Mater. Interfaces* **10**, 44760–44767 (2018).
25. Tsangaris, G. M., Psarras, G. C. & Kouloumbi, N. Electric modulus and interfacial polarization in composite polymeric systems. *J. Mater. Sci.* **33**, 2027–2037 (1998).
26. Davis, J., Hsieh, Y.-H. & Lee, H.-C. Humans perceive flicker artifacts at 500 Hz. *Sci. Rep.* **5**, 7861 (2015).
27. Bredol, M. & Schulze Dieckhoff, H. Materials for powder-based AC-electroluminescence. *Materials* **3**, 1353–1374 (2010).
28. Stauffer, F. & Tybrandt, K. Bright stretchable alternating current electroluminescent displays based on high permittivity composites. *Adv. Mater.* **28**, 7200–7203 (2016).
29. Cordier, P., Tournilhac, F., Soulié-Ziakovic, C. & Leibler, L. Self-healing and thermoreversible rubber from supramolecular assembly. *Nature* **451**, 977–980 (2008).
30. Li, S., Peele, B. N., Larson, C. M., Zhao, H. & Shepherd, R. F. A stretchable multicolor display and touch interface using photopatterning and transfer printing. *Adv. Mater.* **28**, 9770–9775 (2016).
31. Shepherd, R. F., Stokes, A. A., Nunes, R. M. D. & Whitesides, G. M. Soft machines that are resistant to puncture and that self seal. *Adv. Mater.* **25**, 6709–6713 (2013).
32. Rich, S. I., Wood, R. J. & Majidi, C. Untethered soft robotics. *Nat. Electron* **1**, 102–112 (2018).
33. Markvicka, E. J., Bartlett, M. D., Huang, X. & Majidi, C. An autonomously electrically self-healing liquid metal–elastomer composite for robust soft-matter robotics and electronics. *Nat. Mater*. https://doi.org/10.1038/s41563-018-0084-7 (2018).

Methods

Materials. Fluoroelastomer poly(vinylidene fluoride-co-hexafluoropropene) (P(VDF-HFP), 3 M) was used as received, and fluorosurfactant Zonyl FS300 (abcr) was dried in an oven at 70 °C prior to use. The self-healing electrode consists of the same fluoroelastomer and an ionic liquid, 1-ethyl-3-methylimidazolium bis(trifluoromethylsulfonyl) imide (EMITFSI).

Fabrication of the HELIOS device. The dielectric was prepared by mixing 8 g of P(VDF-HFP) with 374 µl of Zonyl FS300 (5 wt%) in 30 ml of acetone and stirred. The solution was poured into a glass petri dish, and the acetone evaporated to form a film that was 1 mm thick. The HELIOS electrode was prepared by mixing 8 g of P(VDF-HFP) with 2.25 ml of EMITFSI in 30 ml of acetone[13]. The solution was stirred and cast in the same way as the dielectric. The dielectric-EL layer was prepared by mixing the combined P(VDF-HFP), Zonyl FS300 and acetone with EL phosphor microparticles (Lonco) using a SpeedMixer (FlackTek), followed by doctor-blade coating to form samples that were 65 µm to 1.5 mm thick. Phosphor microparticles at 20 wt% (9.1 v./v.%), 50 wt% (28.7 v./v.%) and 70 wt% (48.4 v./v.%) were mixed into the dielectric material. The HELIOS device was fabricated by sandwiching the dielectric-EL composite between two electrode layers. Aluminium tape, silver paste, liquid metal or the HELIOS electrode was used to electrically connect the electrode with the external power source.

Materials characterization. The dielectric constants were measured using the Alpha-A high-performance frequency analyser (Novocontrol Technologies). FTIR-ATR measurements were performed on a VERTEX 80v spectrometer (Bruker) from 600 to 4,000 cm^{-1}. Tensile tests were conducted following the American Society for Testing and Materials (ASTM) standard D638 by using Type V tensile bar specimens with 7.62 cm (gauge length) × 3.18 cm (width), tested on an Instron 5900R coupled with a video extensometer. Five samples were tested using a 10 N load cell and stretched at a rate of 1 mm s^{-1}. All the tests above were conducted at room temperature. Nominal stress ($\sigma_{nominal}$) is the applied load on the sample divided by the original cross-sectional area. Nominal strain ($\varepsilon_{nominal}$) is the amount of deformation divided by the initial length of the sample. True stress (σ_{true}) and true strain (ε_{true}) are computed considering the instantaneous dimensions of the samples, where $\sigma_{true} = \sigma_{nominal}(1 + \varepsilon_{nominal})$ and $\varepsilon_{true} = \ln(1 + \varepsilon_{nominal})$. Healing experiments were performed at room temperature (unless otherwise stated) by pressing the damaged interfaces back into contact with a force of ~0.08 N. Interfacial bonding of materials was studied using the T-peel test. The test was conducted using samples of size 1 mm (thickness) × 1 cm (width) × 4 cm (length) each. Two-layered specimens were prepared by gently placing one sample on top of the other sample, with an adherence region of 1 cm (width) × 3 cm (length). Clamped on the tensile tester was 5 mm of the unadhered region of each layer, and the two-layered specimens were pulled at a rate of 1 mm s^{-1}, tested on an Instron 5569. The tests were conducted at room temperature immediately after the two surfaces attached to each other.

DFT calculations. We performed first-principles calculations using the Vienna ab initio simulation package (VASP)[34]. The dispersive forces associated with the van der Waals interaction are treated within the DFT-D2 scheme. The degree of the strength of the interaction of the polymers was estimated by calculating the binding energy, E_b, by building atomic models with periodic boundary conditions. In the VASP, the effect of the images of the molecules was avoided by inserting a vacuum region with a thickness greater than 10 Å. The first Brillouin zone was sampled with a Γ point, and the exchange–correlation functional was adopted with a generalized gradient approximation and Perdew–Burke–Ernzerhof functional. A kinetic energy cutoff of 400 eV was selected for the plane-wave basis set. The structures were fully relaxed until the forces were less than 0.005 eV $Å^{-1}$. As the dipole moment describes the separation of the negative and positive charge centres in a molecule, it scales with and varies with the length of the molecules. For the dipole moment calculation of the HELIOS dielectric, to check the tendency of the charge delocalization in the fluoroelastomer and FS300, we chose their atomic models above with nearly the same length along the chain.

Finite element method simulation. A finite element method solver (COMSOL) was used to study the influence of different κ values of the dielectric materials on the electric field distribution. We used two-dimensional cross-sectional geometries, in which circles represent the EL phosphor powder and are distributed with various densities in different polymers.

Device characterization. Alternating voltage signals (standard sine wave) for activating LECs were generated using NI-cDAQ 9138 programmed through a custom script. The signals were amplified by a high voltage amplifier (Trek 610E), where the V_{ac} values reported are the peak voltages of the sine wave. The luminance values were measured by a luminance meter (TOPCON BM-7), while the illuminance values were measured by a digital light meter HHLM1337 (OMEGA Engineering) placed at a perpendicular distance of 15 mm from the centre of the samples. We defined the turn-on threshold luminance as 0.1 cd m^{-2} because luminance values less than this will be perceived as black by human eyes[35]. The $\eta_{optical}$ was accessed by measuring the luminance at the bifurcated region before and after the healing process. All the optical photographs, when comparing across various samples, were acquired at fixed exposure settings, including the camera settings (ISO, a camera setting that will brighten or darken a photo; aperture settings; and shutter speed). The luminance of the dark box was assumed to be negligible, while the ambient lighting in the lab was measured to be from 15 to 75 lx.

Power measurement was carried out using a modified set-up[6]. Briefly, the resistance of the resistors was measured using a multimeter (72-7780, Tenma Corporation), and the voltage across the resistors was measured via connection to an oscilloscope (KEYSIGHT). In the power test set-up, resistors R_c and R_b are connected in series, and in parallel to the HELIOS device, while R_a is connected in series to the above combination. V_a and V_{ba} are the potential difference across R_a and R_b respectively. The R_a, R_b and R_c were measured to be 21.61 kΩ, 21.66 kΩ and 983 kΩ, respectively. A 200 V, 50 Hz sinusoidal voltage was applied to a sample of approximately 1 cm^2 area and 100 µm thickness. The V_{ba}, V_a and phase shift were read from the graphs plotted from the data to be 4.3 V, 5.2 V and 0.096 rad respectively. The capacitance of the HELIOS device when stretching was measured with an LCR meter (Zurich Instruments). Differential scanning calorimetry and dynamic mechanical analysis measurements were performed on DSC25 and DMA Q800 devices (TA instruments), respectively.

To characterize the f_{sw} and turn-on delay of the HELIOS device, a photodiode (FDS100) was connected to an operational amplifier (LTC1052) to detect the light signal emitted from a Helios device ($V_{ac} = 200$ V, $E = 2$ V μm^{-1}) and an LED ($V = 2.6$ V). The HELIOS device was driven by a composite signal, which is the product of f_{ac} and f_{sw} signals. Both the driving signal and the detected signal were connected to an oscilloscope (KEYSIGHT) for data collection.

Soft robotic gripper. Ecoflex 00-50 (Smooth-On) and 15 wt% cellulose fibers (Sigma Aldrich) were mixed using the SpeedMixer, and the mixture was cured in an acrylic mould to give the top pneumatic network structure. To fabricate the base with the embedded HELIOS devices, a thin layer of Ecoflex 00-50 was cured in a base mould. The HELIOS devices were placed on top of this layer and electrically connected in parallel. The silicone–cellulose mixture was poured over these to fill the base mould and then cured. The base and top pneumatic network structures were then sealed by additional silicone–cellulose mixture. A photodetector (ams TCS3200D, TAOS) was adhered to the centre of the gripper base using Ecoflex 00-50. The soft robot was pneumatically actuated.

Wireless HELIOS. Flexible printed circuit boards (PCBs) integrating the loop antenna and interconnection traces were fabricated. The power harvester was fabricated as follows. The rectifier was assembled on a rigid PCB (R4-TG130 substrate, 1 oz. silver) by microsoldering (NAE-2A, JBC) the following components: (1) a 10 pF capacitor (Johanson Technology), (2) a 10 nF capacitor (Murata Electronics, GRM0335C1HR20WA01D), (3) a 68 pF capacitor (Murata Electronics, GRM0335C1E680JA01) and (4) a Schottky diode (Skyworks, SMS7621-060). The PCBs were integrated together with a yellow LED chip (Lumex) in series with a resistor (Yageo). The power harvester was connected in parallel with a control circuit (fabricated on a flexible PCB, with a dimension of 30 × 30 mm^2) consisting of an EL lamp driver (HV860) to drive the HELIOS device and a control LEC device (made with silicone) (Supplementary Fig. 32). All the flexible PCBs were encapsulated inside a disc above the soft gripper using Ecoflex 00-50. The LEC devices were wirelessly powered using an antenna coil (4 cm in diameter) as a transmitter, driven by a signal generator (SMB100A, Rohde and Schwarz) and a power amplifier (Mini-Circuits) at a radio-frequency signal of 133 MHz.

Data availability

The data that support the findings of this study are available from the authors on reasonable request.

References

34. Kresse, G. & Furthmüller, J. Efficient iterative schemes for ab initio total-energy calculations using a plane-wave basis set. *Phys. Rev. B* **54**, 11169–11186 (1996).
35. Daly, S., Kunkel, T., Sun, X., Farrell, S. & Crum, P. Viewer preferences for shadow, diffuse, specular, and emissive luminance limits of high dynamic range displays. *SID Int. Symp. Dig. Tech.* **44**, 563–566 (2013).
36. Li, C.-H. et al. A highly stretchable autonomous self-healing elastomer. *Nat. Chem.* **8**, 618–624 (2016).

Acknowledgements

B.C.K.T. acknowledges support from the Singapore National Research Fellowship (NRFF2017-08), an NUS Start-up Grant and the Singapore National Robotics Programme (NRP 1822500053). J.Ho acknowledges support from National Research Foundation Singapore (NRFF2017-07) and an NUS Young Investigator Award. We thank Z. Goh for assistance with the illustration in Fig. 1a and W. Lee for photographs in Fig 1b. We thank A. Cheong, X. Tan and H. Li for access to testing equipment.

Author contributions

Y.J.T. and B.C.K.T conceived the idea. B.C.K.T. directed the research activities. Y.J.T. and B.C.K.T. designed and led the experiments (with input from H.G., G.C., S.T.M.T.,

G.X.W., G.L., P.M.L., Y.C., S.L., R.F.S. and J.H.). Y.J.T., H.G., G.C., G.X.W. and B.C.K.T. contributed to data analysis and interpretation. Y.J.T. and B.C.K.T. wrote the paper, and all authors provided feedback.

Competing interests
The authors declare no competing interests.

Additional information
Extended data is available for this paper at https://doi.org/10.1038/s41563-019-0548-4.

Supplementary information is available for this paper at https://doi.org/10.1038/s41563-019-0548-4.

Correspondence and requests for materials should be addressed to B.C.K.T.

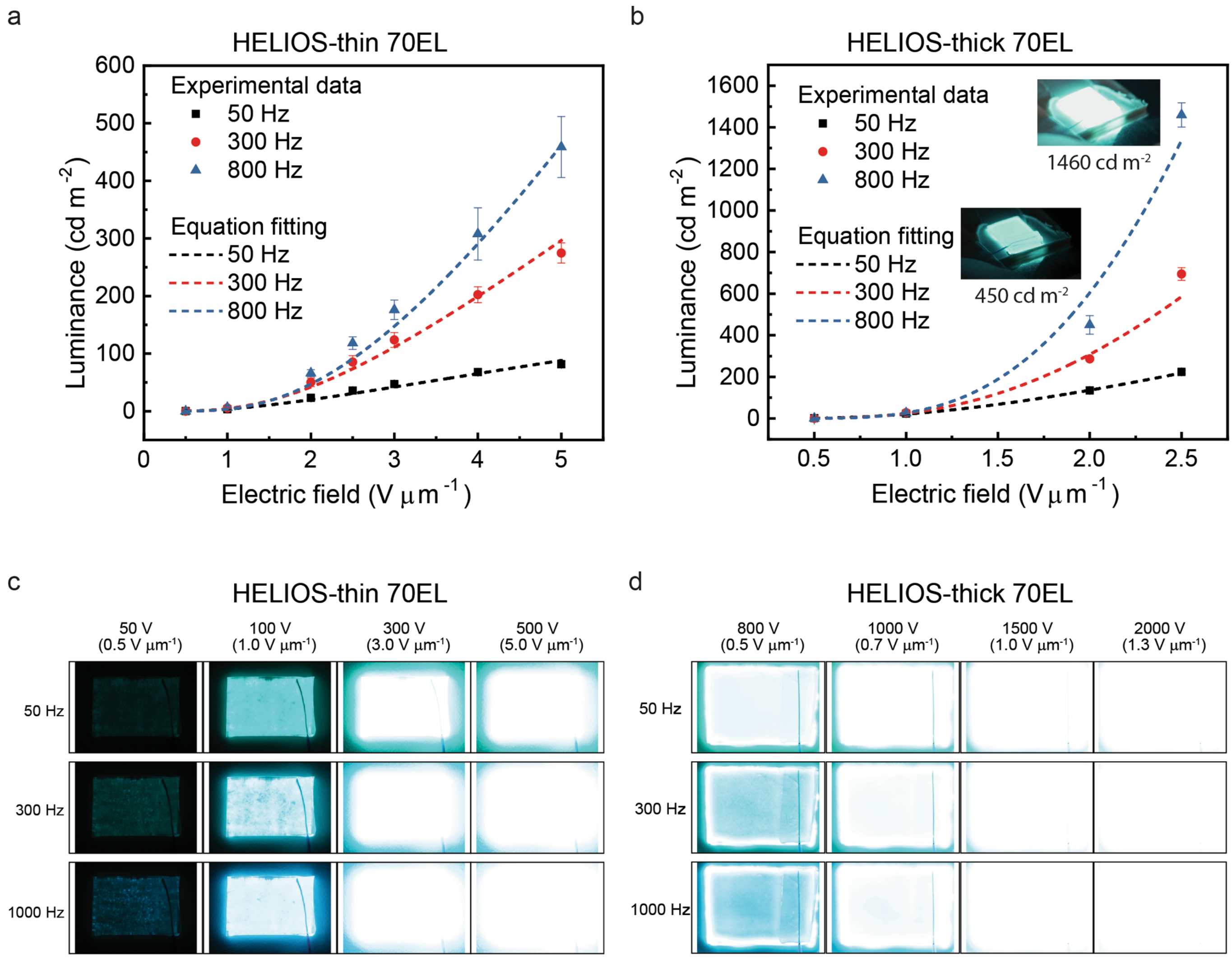

Extended Data Fig. 1 | Thickness effect of dielectric-EL on the brightness of HELIOS 70EL at the same *E* and f_{ac}. (a-b) The brightness of HELIOS 70EL increases with the increase in thickness in the dielectric-EL ($t = 100\,\mu m$ vs $t = 1500\,\mu m$) when comparing with the same ***E*** and frequencies applied. The measurements were repeated on three samples and the error bars represent the standard deviation. The luminance and the operated fields on the HELIOS devices are expressed using the equation of $L = L_o \exp(-b/\boldsymbol{E}^{0.5})$. Insets show the photographs of the oblique view of the HELIOS device. (c-d) Photographs showing that the HELIOS-thick 70EL device is significantly brighter than the HELIOS-thin 70EL device.

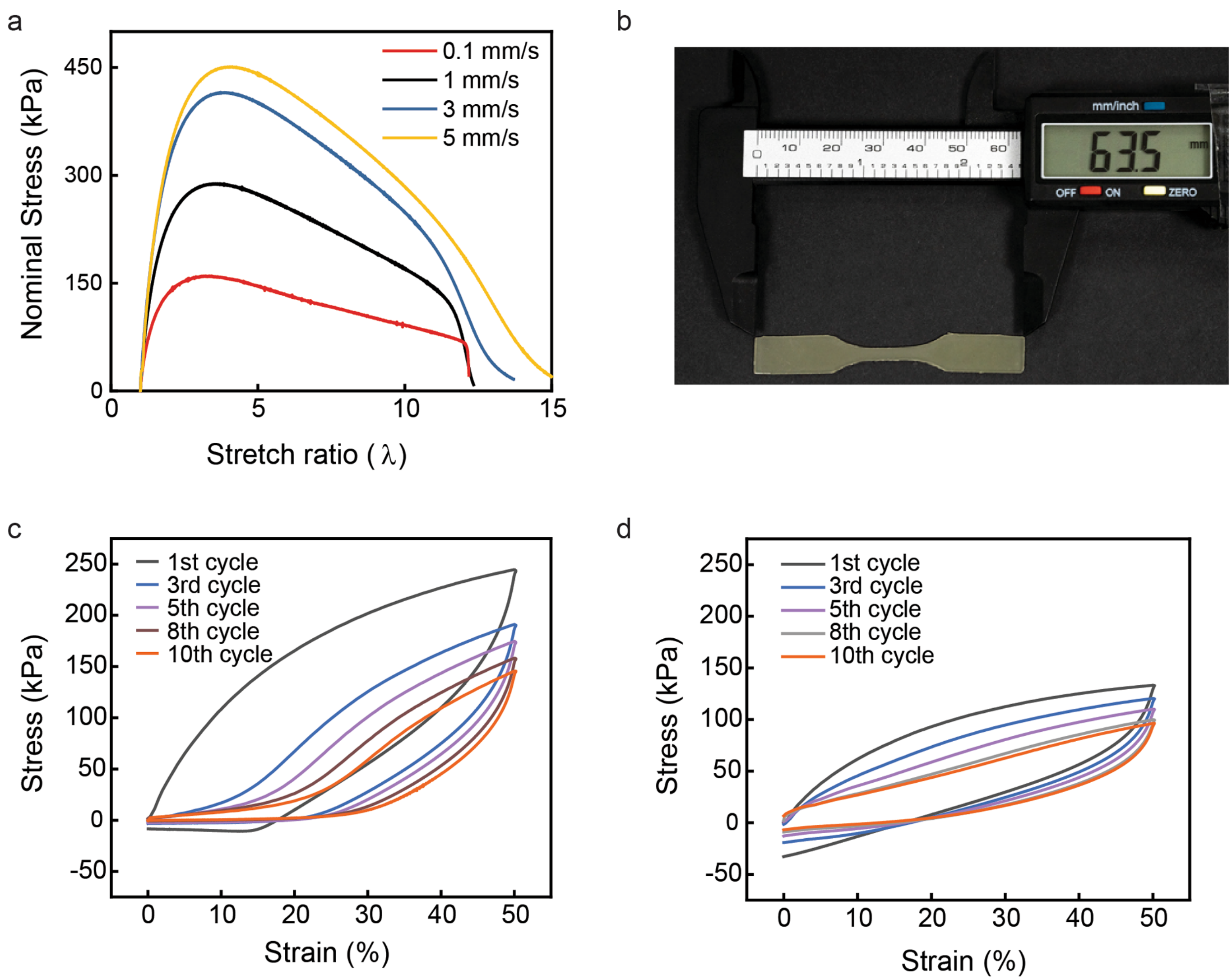

Extended Data Fig. 2 | Mechanical tests. (a) The stress-strain curve of the HELIOS dielectric stretched at different speeds. The modulus increases when stretching at higher speed, which is the typical behaviour of supramolecular polymers[22,36]. (b) Photograph showing tensile bar specimen (Type V) following ASTM standard D638 with 7.62 cm (gauge length) x 3.18 cm (width). (c) Dielectric-EL sample and (d) three-layered HELIOS device samples were subjected to ten loading-unloading cycles (loading at 1 mm s^{-1} and unloading at 1 mm min^{-1}). These materials recovered to its original length when subjected to a strain of 50% over time.

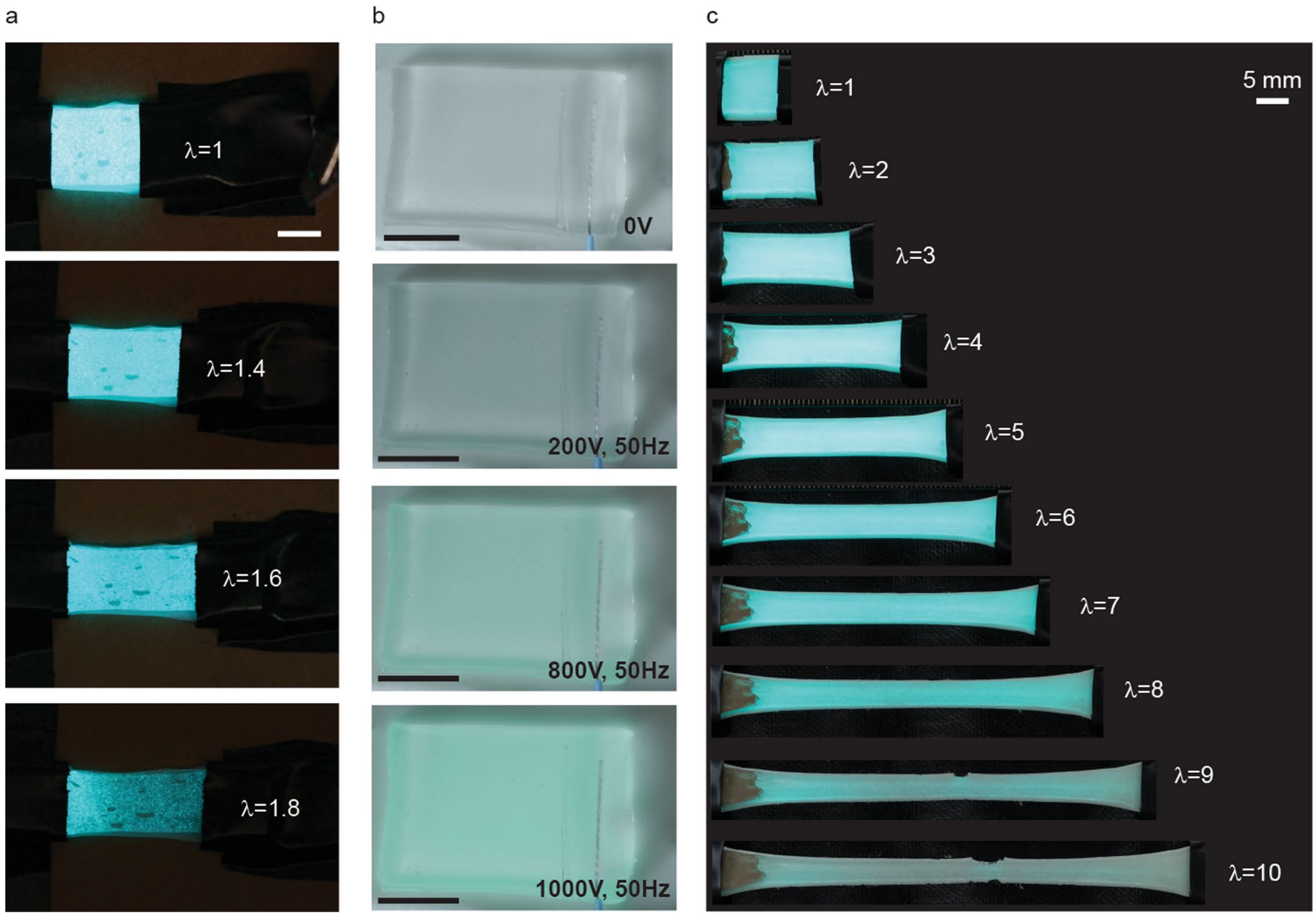

Extended Data Fig. 3 | Demonstration of HELIOS-thin (t = 67 μm) vs HELIOS-thick (t = 1 mm) LEC devices stretched to various strains. (a) HELIOS-thin can stretch to ~1.6 times its original length. Scale bar: 5 mm. (b) Photographs showing that HELIOS-thick activated at f_{ac} of 200 V and 50 Hz (vaguely visible), and the device is bright when operated at 800 V (and 1000 V) and f_{ac} of 50 Hz when operated under daylight condition. Scale bar: 5 mm. (c) The HELIOS-thick device stretches with an increase in light emission and subsequently exhibited stable illumination up to 9 times its original length.